Velocity Profiles in Repulsive Athermal Systems under Shear

Ning Xu,[1] Corey S. O'Hern,[1,2] and Lou Kondic[3]

[1]*Department of Mechanical Engineering, Yale University, New Haven, Connecticut 06520-8284, USA*
[2]*Department of Physics, Yale University, New Haven, Connecticut 06520-8120, USA*
[3]*Department of Mathematical Sciences, New Jersey Institute of Technology, Newark, New Jersey 07102, USA*

(Received 1 March 2004; published 5 January 2005)

We conduct molecular dynamics simulations of athermal systems undergoing boundary-driven planar shear flow in two and three spatial dimensions. We find that these systems possess nonlinear mean velocity profiles when the velocity u of the shearing wall exceeds a critical value u_c. Above u_c, we also show that the packing fraction and mean-square velocity profiles become spatially dependent with dilation and enhanced velocity fluctuations near the moving boundary. In systems with overdamped dynamics, u_c is only weakly dependent on packing fraction ϕ. However, in systems with underdamped dynamics, u_c is set by the speed of shear waves in the material and tends to zero as ϕ approaches ϕ_c, which is near random close packing at small damping. For underdamped systems with $\phi < \phi_c$, u_c is zero; thus they possess nonlinear velocity profiles at any nonzero u.

DOI: 10.1103/PhysRevLett.94.016001 PACS numbers: 83.50.Ax, 45.70.Mg, 64.70.Pf, 83.10.Rs

Driven, dissipative systems are ubiquitous in nature (occurring much more frequently than equilibrium thermal systems) and display complex behaviors in response to applied loads, such as hysteretic and spatially dependent flows. Many of these systems such as granular materials [1,2], metallic glasses [3], and complex fluids, for example, emulsions [4], foams [5,6], and wormlike micelles [7], do not flow homogeneously with a linear velocity profile when they are sheared. Shear localization or banding can occur where a small fraction of the system near one of the boundaries undergoes strong shear flow while the remainder of the system is nearly static. Despite much intense work, a complete description of how these systems respond to shear stress is not available. We perform molecular dynamics (MD) simulations of repulsive athermal particulate systems in two (2D) and three (3D) spatial dimensions undergoing boundary-driven planar shear flow to study mechanisms that give rise to spatially inhomogeneous velocity profiles. These studies will be most relevant to shear flows in athermal systems, such as granular materials and foams.

We answer several important questions in this Letter. First, does the packing fraction of the system strongly influence the shape of the velocity profiles? Most previous simulations investigating velocity profiles in sheared systems have been performed either near random close packing as in simulations of granular materials [8] or at high density as in studies of Lennard-Jones liquids [9] and glasses [10,11]. However, a systematic study of the role of density has not been performed. Nonlinear velocity profiles have been found at both high density and near random close packing, but it is not clear whether the same physical mechanism is responsible in both regimes.

We also consider the influence of the speed u of the shearing boundary on the velocity profiles. Results from previous simulations of glassy systems [10,11] indicate that a critical velocity u_0 exists below which the mean velocity profiles become nonlinear [12]. These studies have found that u_0 coincides with the velocity at which the constant velocity flow curve falls below the yield stress at constant stress. In this Letter, we concentrate on the larger u regime and ask whether the velocity profiles remain linear for all $u > u_0$. We show that a different transition takes place—the velocity profile switches from linear to nonlinear—when the boundary velocity exceeds $u_c \geq u_0$. The onset of nonlinear velocity profiles at large u also coincides with the appearance of nonuniform packing fraction and temperature profiles. The flow regimes are depicted in Fig. 1 using the flow curve for an underdamped athermal system in 2D.

To demonstrate these results, we performed a series of molecular dynamics simulations of soft repulsive athermal systems undergoing boundary-driven shear flow under

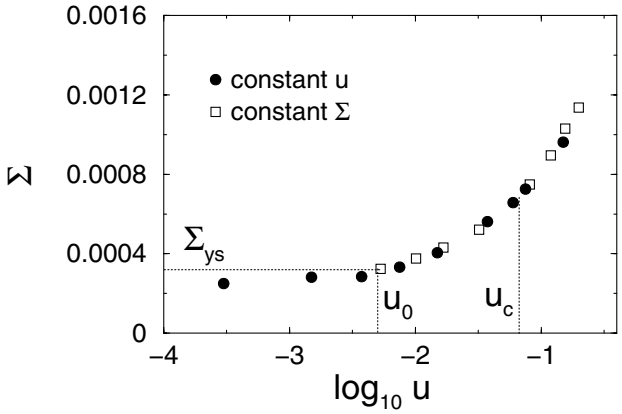

FIG. 1. Shear stress Σ vs velocity u of the wall moving at constant velocity (circles) or stress (squares) for a 2D underdamped athermal system with harmonic spring interactions at $\phi = 0.85$. Σ_{ys} is the yield stress at constant stress and u_0 is the wall velocity at which $\Sigma = \Sigma_{ys}$. We show later that the mean velocity profiles become nonlinear when $u > u_c$.

conditions of fixed volume, number of particles N, and velocity of the top shearing wall u. The systems were composed of $N/2$ large and $N/2$ small particles with equal mass m and diameter ratio 1.4 to prevent crystallization and segregation. Initial states were prepared by quenching the system from random initial positions to zero temperature [13] using the conjugate gradient method [14] to minimize the system's total potential energy. During the quench, periodic boundary conditions were implemented in all directions. Following the quench, particles with y coordinates $y > L_y$ ($y < 0$) were chosen to comprise the top (bottom) boundary. The walls were therefore rough and amorphous. Results did not depend on the thermal quench rate provided the systems were sheared long enough to remove initial transients.

Shear flow in the x direction with a shear gradient in the y direction was created by moving all particles in the top wall at fixed velocity u in the x direction relative to the stationary bottom wall. Therefore, particles in the walls do not possess velocity fluctuations. During the shear flow, periodic boundary conditions were imposed in the x and z directions (in 3D). The system size was varied in the range $N = [256, 3072]$ to assess finite-size effects. Only small sample sizes were required in the x and z directions. In contrast, more than ≈ 50 particle layers were required in the shear-gradient direction to remove finite-size effects. Most simulations were carried out using $L_x = L_z = 18\sigma$ and $L_y = 72\sigma$, where σ is the small particle diameter. The systems were sheared for a strain of 5 to remove initial transients and then quantities like velocity, pressure, and shear stress (obtained from the ''microscopic'' pressure tensor [15]) and local packing fraction were measured as a function of distance y from the stationary wall. Averaged quantities were obtained by sampling between strains of 5 to 10.

Bulk and boundary particles interact via the following pairwise, finite-range, purely repulsive potential: $V(r_{ij}) = \epsilon(1 - r_{ij}/\sigma_{ij})^\alpha/\alpha$, where $\alpha = 2, 5/2$ correspond to harmonic and Hertzian spring interactions, respectively, ϵ is the characteristic energy scale of the interaction, $\sigma_{ij} = (\sigma_i + \sigma_j)/2$ is the average diameter of particles i and j, and r_{ij} is their separation. The interaction potential is zero when $r_{ij} \geq \sigma_{ij}$. Our results were obtained over a range of packing fraction from $\phi = [0.58, 0.80]$ in 3D and $\phi = [0.75, 1.0]$ in 2D, which allows us to probe packing fractions both above and below random close packing [13]. The units of length, energy, and time are σ, ϵ, and $\sigma\sqrt{m/\epsilon}$, respectively.

For athermal or dissipative dynamics, the position and velocity of each particle are obtained by solving [16]

$$m\frac{d^2\vec{r}_i}{dt^2} = \vec{F}_i^r - b\sum_j(\vec{v}_i - \vec{v}_j), \tag{1}$$

where $\vec{F}_i^r = -\sum_j dV(r_{ij})/dr_{ij}\hat{r}_{ij}$, the sums over j include only particles that overlap i, $\vec{v}_i$ is the velocity of particle i, and $b > 0$ is the damping coefficient. In the present study we do not consider rotational motion of the particles; the influence of the rotational degrees of freedom on the velocity profiles will be discussed elsewhere [17]. The dynamics can be changed from underdamped to overdamped by increasing the dimensionless damping coefficient $b^* = b\sigma/\sqrt{\epsilon m}$. Frictionless granular materials and model foams can be studied using $b^* < b_c^*$ [16] and $b^* \gg b_c^*$ [18], respectively, where $b_c^* = \sqrt{2}$ for harmonic spring interactions.

Three physical parameters, the packing fraction ϕ, the velocity u of the moving boundary, and the dimensionless damping coefficient b^*, strongly influence the shape of the mean velocity profiles. First, we find that a critical boundary velocity u_c exists that separates linear from nonlinear flow behavior. For $u < u_c$ (but not in the quasistatic flow regime), the mean velocity profiles in the flow direction are linear; however, when $u > u_c$ they become nonlinear. The width of the shearing region decreases as u continues to increase above u_c. This is shown in Fig. 2(a) for an underdamped ($b^* \ll b_c^*$) system in 2D with harmonic spring interactions at $\phi = 0.85$. As u is increased above $u_c \approx 0.08$, the mean velocity profiles become more and more nonlinear. When the boundary velocity has increased to $u = 0.75$ in Fig. 2(a), approximately 80% of the system is nearly static, while the remaining 20% undergoes shear flow.

We also monitored the local packing fraction and mean-square velocity fluctuations (or kinetic temperature) during shear. These are shown for the same dense system with underdamped dynamics in Figs. 2(b) and 2(c). We find that when the mean velocity profile is linear, the packing fraction and velocity fluctuations are spatially uniform. Moreover, the velocity fluctuations in the x and y directions are identical. However, when the boundary velocity exceeds u_c, the packing fraction and mean-square velocity profiles become spatially dependent. In this regime, the compressional forces induced by the shearing boundary are large enough to cause dilatancy. The system becomes less dense near the shearing wall and more compact in the nearly static region. In addition, the shearing wall induces a kinetic temperature gradient with velocity fluctuations larger near the shearing boundary. The kinetic temperature also becomes anisotropic with $\langle \delta v_x^2 \rangle < \langle \delta v_y^2 \rangle$ when $u > u_c$. Thus, several phenomena occur simultaneously as the boundary velocity is increased above u_c: (i) the velocity profile becomes nonlinear, (ii) the system dilates near the shearing boundary and compacts in the bulk, and (iii) the kinetic temperature becomes higher near the shearing wall.

We have measured the critical wall velocity u_c as a function of packing fraction ϕ for underdamped systems with harmonic and Hertzian spring interactions in 2D and 3D. To calculate u_c, we successively lowered the boundary velocity from above until the average velocity profile of the central region of the cell ($y/L_y = [0.2, 0.8]$) was within

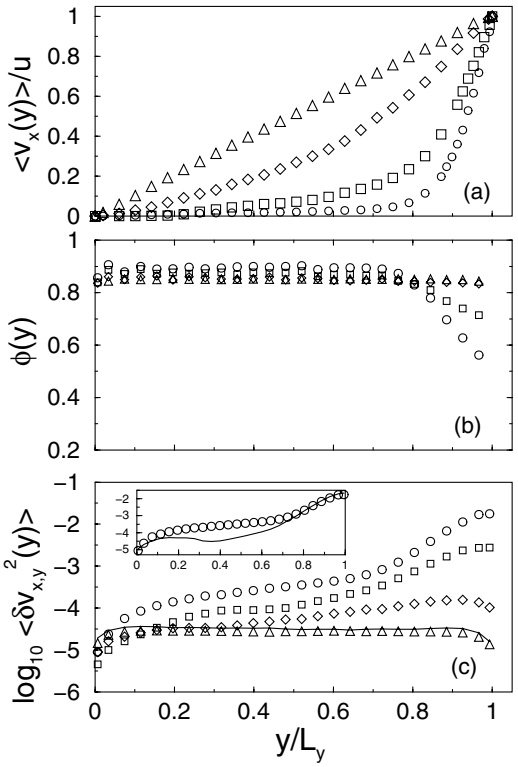

FIG. 2. (a) Average velocity $\langle v_x \rangle$ (normalized by u) in the flow direction, (b) local packing fraction ϕ, and (c) velocity fluctuations $\langle \delta v_{x,y}^2 \rangle$ in the x (solid lines) and y directions (symbols) as a function of height y/L_y from the stationary wall in a 2D system with harmonic spring interactions and underdamped dynamics ($b^* = 0.01$) at $\phi = 0.85$. In each panel, four boundary velocities are shown; triangles, diamonds, squares, and circles correspond to $u = 0.075$, 0.15, 0.37, and 0.75, respectively. The inset to (c) compares velocity fluctuations in the x and y directions at $u = 0.75$.

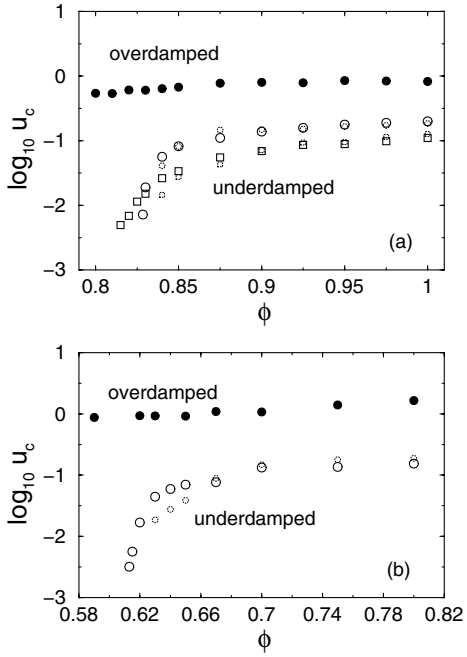

FIG. 3. Critical velocity u_c of the moving wall versus packing fraction ϕ in (a) 2D and (b) 3D systems with harmonic (circles) and Hertzian (squares) spring interactions. The open and filled symbols correspond to $b^* = 0.01$ and $b^* = 5$, respectively. For underdamped systems, we plot $u_T/2$ for harmonic (small circles) and Hertzian (small squares) spring interactions, where u_T is the shear wave speed.

rms velocity fluctuations of a linear profile. As shown in Fig. 3, we find that u_c is nearly constant at large ϕ but then decreases sharply as ϕ approaches a critical packing fraction ϕ_c [19]. For $\phi < \phi_c$, $u_c = 0$ with $\phi_c \approx 0.82$ for harmonic and $\phi_c \approx 0.80$ for Hertzian springs in 2D and $\phi_c \approx 0.61$ for harmonic springs in 3D. We expect qualitatively similar behavior for u_c for Hertzian springs in 3D with a ϕ_c that is a few percent below that for harmonic springs in 3D. These values for ϕ_c are close to recent measurements of random close packing in systems at zero temperature [13].

A possible interpretation of the critical wall velocity u_c can be obtained by comparing the time it takes the system to shear a unit strain to the time it takes a shear wave (with speed u_T) to traverse the system and return to the shearing boundary. This simple argument predicts $u_c = u_T/2$. u_T can be obtained by studying the transverse current correlation function $C_T(\omega, k)$ as a function of frequency ω and wave number $k = 2\pi n\sigma/L_x$ (n = integer) and the resulting dispersion relation $\omega_T(k)$ [20]. In Fig. 3, we compare $u_T = d\omega_T/dk$ (for $n = 3$ to 12) and u_c as a function of ϕ for both potentials in 2D and for harmonic springs in 3D [21]. Although deviations occur close to ϕ_c, we find that u_c agrees very well with $u_T/2$ over a wide range of ϕ. We point out that $u_c \sim u_T$ tends to zero as ϕ approaches random close packing. Thus, we expect the mechanism for nonlinear velocity profiles described here to occur in experiments on even moderately sheared granular systems. Measurements of u_c and u_T in granular systems undergoing planar shear flow are required to verify this.

What is the shape of velocity profiles in dilute underdamped systems with $\phi < \phi_c$? Since $u_c = 0$ for $\phi < \phi_c$, we expect that mean velocity profiles in these dilute systems are nonlinear for all nonzero u. This is indeed what we find for all systems studied. Figure 4 shows the mean velocity profiles for a 2D underdamped system at $\phi < \phi_c$ over three decades in u. In contrast to the behavior in dense systems, the velocity profiles are not monotonic in u. However, there is a range of boundary velocities (one decade) over which the velocity profiles collapse onto a common exponential profile over 70% of the system. Robust exponential profiles have also been found over a wide range of shear rates in experiments of granular materials [2]. Spatially dependent packing fraction and mean-square velocity profiles also occur for all $u \neq 0$.

Boundary-driven shear flow in *overdamped* systems is, however, substantially different from that in underdamped systems since velocities of neighboring particles are strongly coupled. Figure 3 shows that in the overdamped limit ($b^* \gg b_c^*$), the critical boundary velocity is nearly

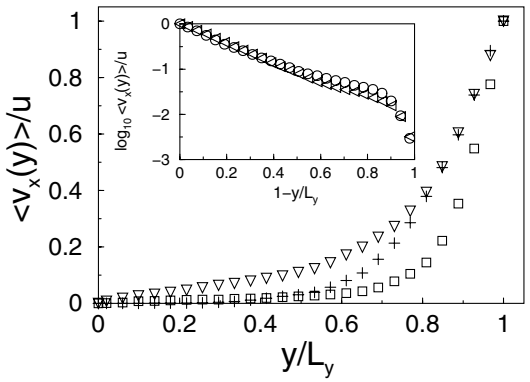

FIG. 4. Average velocity $\langle v_x\rangle/u$ in the shear flow direction as a function of height y/L_y from the stationary wall in a 2D underdamped system with harmonic spring interactions at $\phi = 0.81 < \phi_c$. Three boundary velocities are shown; squares, downward triangles, and pluses correspond to $u = 0.38$, 0.038, and 7.7×10^{-4}, respectively. The inset shows that there is a wide range of u from 0.0077 (leftward triangles) to 0.077 (circles) over which the velocity profiles collapse.

independent of ϕ over the studied range in both 2D and 3D. We also find that u_c increases linearly with b^*; thus the velocity profiles tend toward linear profiles as the damping increases at fixed u.

We have also studied sheared repulsive systems thermostated at temperatures below the glass transition using the Gaussian constraint thermostat on velocity components perpendicular to the shear flow [15] to determine whether our results also hold for glasses. We find qualitatively similar results to those found in *underdamped* athermal repulsive systems; i.e., we find that velocity profiles switch from linear to nonlinear when u increases above u_c, where u_c is set by the shear wave speed. We also find dilatancy and breakdown of equipartition when $u > u_c$. We have confirmed these results for harmonic spring interactions at densities above and below random close packing, in 2D and 3D, and over a range of temperatures below the glass transition [17].

In this Letter we present results of MD simulations of repulsive athermal systems undergoing boundary-driven shear flow in 2D and 3D. We demonstrate that a critical boundary velocity u_c exists that signals the onset of spatial inhomogeneity at large u. When $u > u_c$, the mean velocity profiles become nonlinear, the system becomes dilated near the moving wall and compressed near the stationary wall, and the system possesses a nonuniform kinetic temperature profile with higher temperature near the moving wall. For underdamped systems, u_c is nearly constant at large ϕ but decreases strongly at lower ϕ until it vanishes at ϕ_c. Below ϕ_c, the velocity profiles are nonlinear for all $u > 0$. In the underdamped limit, u_c is determined by the shear wave speed u_T. Initial studies indicate that these results for underdamped systems also hold for repulsive glasses. However, in the overdamped limit u_c is nearly independent of ϕ over the studied range and scales linearly with the damping coefficient.

We thank R. Behringer, A. Liu, and M. Robbins for helpful comments. Financial support from NASA Grants No. NAG3-2377 (N. X.) and No. NNC04GA98G (L. K.) and Yale University (N. X., C. S. O.) is gratefully acknowledged.

[1] D. M. Mueth, G. F. Debregeas, G. S. Karczmar, P. J. Eng, S. R. Nagel, and H. M. Jaeger, Nature (London) **406**, 385 (2000).
[2] W. Losert, L. Bocquet, T. C. Lubensky, and J. P. Gollub, Phys. Rev. Lett. **85**, 1428 (2000); D. Howell, R. P. Behringer, and C. Veje, Phys. Rev. Lett. **82**, 5241 (1999).
[3] X. Fu, D. A. Rigney, and M. L. Falk, J. Non-Cryst. Solids **317**, 206 (2003).
[4] P. Coussot, J. S. Raynaud, F. Bertrand, P. Moucheront, J. P. Guilbaud, H. T. Huynh, S. Jarny, and D. Lesueur, Phys. Rev. Lett. **88**, 218301 (2002).
[5] G. Debregeas, H. Tabuteau, and J.-M di Meglio, Phys. Rev. Lett. **87**, 178305 (2001).
[6] J. Lauridsen, G. Chanan, and M. Dennin, Phys. Rev. Lett. **93**, 018303 (2004).
[7] J.-B. Salmon, A. Colin, S. Manneville, and F. Molino, Phys. Rev. Lett. **90**, 228303 (2003).
[8] P. A. Thompson and G. S. Grest, Phys. Rev. Lett. **67**, 1751 (1991).
[9] S. Y. Liem, D. Brown, and J. H. R. Clarke, Phys. Rev. A **45**, 3706 (1992).
[10] F. Varnik, L. Bocquet, J.-L. Barrat, and L. Berthier, Phys. Rev. Lett. **90**, 095702 (2003).
[11] J. Rottler and M. O. Robbins, Phys. Rev. E **68**, 011507 (2003).
[12] Preliminary results on the systems considered here show that *instantaneous* velocity profiles are indeed nonlinear for $u < u_0$, but more work needs to be done to fully characterize the mean profiles.
[13] C. S. O'Hern, S. A. Langer, A. J. Liu, and S. R. Nagel, Phys. Rev. Lett. **88**, 075507 (2002); C. S. O'Hern, L. E. Silbert, A. J. Liu, and S. R. Nagel, Phys. Rev. E **68**, 011306 (2003).
[14] W. H. Press, B. P. Flannery, S. A. Teukolsky, and W. T. Vetterling, *Numerical Recipes in Fortran 77* (Cambridge University Press, New York, 1986).
[15] D. J. Evans and G. P. Morriss, *Statistical Mechanics of Nonequilibrium Liquids* (Academic Press, London, 1990).
[16] S. Luding, Phys. Rev. E **55**, 4720 (1994).
[17] N. Xu and C. S. O'Hern (unpublished).
[18] D. J. Durian, Phys. Rev. E **55**, 1739 (1997).
[19] u_0 also decreases strongly near random close packing, but for all systems studied $u_0 \leq u_c$. In particular, we find that when $u_c = 0$, $u_0 = 0$ also.
[20] J. P. Hansen and I. R. McDonald, *Theory of Simple Liquids* (Academic Press, London, 1986).
[21] To simplify the calculations, we measured $u_T(\phi)$ in low-temperature, quiescent reference systems. This is justified because the ϕ contribution to u_T is much larger than the fluctuation contribution to u_T for systems with ϕ above random close packing and $u \sim u_c$.